

First-Principles Study of Fe-Mo Double Perovskites

E. Carvajal^a, R. Oviedo-Roa^b, M. Cruz-Irisson^a, and O. Navarro^{c,d}

^a*Instituto Politécnico Nacional, ESIME-Culhuacán*

Av. Santa Ana 1000, C.P. 04430, México, D.F., México.

^b*Programa de Investigación en Ingeniería Molecular, Instituto Mexicano del Petróleo, Eje Central Lázaro Cárdenas Norte 152, C.P. 07730, México D.F., México.*

^c*Instituto de Investigaciones en Materiales, Universidad Nacional Autónoma de México, A.P. 70-360, 04510 México, D.F., México.*

^d*Instituto de Investigaciones Metalúrgicas, Universidad Michoacana de San Nicolás de Hidalgo, Edificio "U" Ciudad Universitaria, 58000 Morelia Michoacán, México.*

e-mail: ecarvajalq@ipn.mx

Recibido el 25 de junio de 2010; aceptado el 6 de octubre de 2010

We have studied the $\text{Sr}_2\text{Fe}_{1+x}\text{Mo}_{1-x}\text{O}_6$ compound using first-principles density functional theory. The calculations were done within the generalized gradient approximation scheme and with the Perdew-Burke-Ernzerhof functional. A detailed analysis on the bonding or antibonding character of the Fe and Mo orbitals together with the distribution and the way of hybridization of those orbitals in the valence and conduction bands has been done. Our spin-polarized calculations for the tetragonal lattice, where Mo sites have been replaced with Fe in the ordered structure, give a half-metallic ground state for $x > 0$.

Keywords: Double perovskites; magnetoresistance; first-principles.

Hemos estudiado el compuesto $\text{Sr}_2\text{Fe}_{1+x}\text{Mo}_{1-x}\text{O}_6$ usando la teoría de las funcionales de la densidad de primeros principios. Los cálculos fueron hechos dentro del esquema de la aproximación del gradiente generalizado, utilizando la funcional de Perdew-Burke-Ernzerhof. Se ha hecho un análisis detallado del carácter enlazante o antienlazante de los orbitales del Fe y el Mo junto con la distribución y la manera en que se hibridizan estos orbitales en las bandas de valencia y conducción. En nuestros cálculos con espín polarizado para la red tetragonal, donde sitios de Mo han sido reemplazados con Fe en la estructura ordenada, se obtiene un estado base medio metálico para $x > 0$.

Descriptor: Perovskitas dobles; magnetorresistencia; primeros principios.

PACS: 71.15.Mb; 71.30.+h; 72.25.-b; 71.23.-k

1. Introduction

The study of electronic transport and magnetotransport of new materials is of great interest since new phenomena and potential applications may be discovered. Particularly, the phenomenon of colossal magnetoresistance (CMR) shown by the manganese-based and other analogous compounds is very interesting. Manganites crystallize in the cubic structure of the perovskite mineral CaTiO_3 and it was found that a magnetic transition is accompanied by a metal-insulator transition for hole-doped manganese oxides. However, they do not share the model to explain the electromagnetic behavior with other colossal magnetoresistive materials, as some pyrochlores or spinels. Some attempts to clarify the physical processes involved in the CMR were made studying the effect of doping on the manganites. The spot light was put on CMR after the measurements reported by Kobayashi *et al.* [1] on the oxide compound $\text{Sr}_2\text{FeMoO}_6$, which shows a double perovskite structure and magnetoresistance at room temperature. Fundamental and practical interests have guided the research since then because of the possible commercial applications from magnetic sensors to electrodes in solid-oxide fuel cells. Experimental studies provided a lot of information on $\text{Sr}_2\text{FeMoO}_6$, obtained by multiple techniques, *e.g.*, neutron diffraction [2], nuclear magnetic resonance [3], electron

spin resonance [4] and X-ray absorption, ultraviolet photoelectron and electron energy-loss spectroscopies [5] among others. As a result of all the experimental contributions, it is known that $\text{Sr}_2\text{FeMoO}_6$ is a half-metallic ferromagnetic oxide with complete spin polarization and substantial low-field magnetoresistance. The Fe-Mo compound is a potential candidate for memory devices because of its fairly high Curie temperature. Changes in composition of the double perovskite $\text{Sr}_2\text{FeMoO}_6$ modify radically its physical properties. The best example is Sr_2FeWO_6 [6] that is an antiferromagnetic insulator. Mis-site disorder and its effects on the conduction band are also very important to explain electronic and magnetic properties of this double perovskite. There have been some efforts to study the effects of disorder and the electronic correlation [7,8]. However, in view of the difficulty to have a detailed control of mis-site disorder effect we follow the route introduced early by Topwal *et al.* [9] to investigate the off-stoichiometric $\text{Sr}_2\text{Fe}_{1+x}\text{Mo}_{1-x}\text{O}_6$ system. In this paper, we study the $\text{Sr}_2\text{Fe}_{1+x}\text{Mo}_{1-x}\text{O}_6$ double perovskite for $x > 0$, here the system is rich in Fe since some Mo's are replaced with Fe in the ordered structure. We study the evolution of the density of states using density functional theory (DFT) calculations and changing the Fe/Mo relative content in a supercell.

2. Methods and computational details

The electronic properties of $\text{Sr}_2\text{Fe}_{1+x}\text{Mo}_{1-x}\text{O}_6$ were studied within the DFT framework. We used the generalized gradient approximation (GGA) with the PBE functional [10], within the CASTEP code [11, 12], as implemented in the Materials Studio software suite. To study the different compositions of $\text{Sr}_2\text{Fe}_{1+x}\text{Mo}_{1-x}\text{O}_6$ we constructed a 160 atoms supercell which was made up by eight unit cells ($2 \times 2 \times 2$), where two stoichiometric formula units ($\text{Sr}_2\text{FeMoO}_6$) are contained in each one. In the starting supercell of $\text{Sr}_2\text{FeMoO}_6$ (Fig. 1) the Mo atoms were replaced by Fe atoms systematically, to built up each one of the supercells.

The lowest concentration of Fe in our supercells corresponds to $x = 0$ ($\text{Sr}_2\text{FeMoO}_6$) in the $\text{Sr}_2\text{Fe}_{1+x}\text{Mo}_{1-x}\text{O}_6$ compound and it is found in the Mo-O-Fe-O-Mo-O-Fe-O-chains along the $[0\ 0\ 1]$ direction. Subsequent replacement of Mo atoms by Fe translates into a kind of control of both: the order and the relative concentration. In the first generated supercell (A) a Mo atom was replaced by Fe, so that one of the mentioned chains transforms into Mo-O-Fe-O-Fe-O-Fe-O- without perturbing the other ones and there is now 6.25% more Fe than Mo. The second supercell (B) contains one more Fe atom than the previous one so that one of all the possible chains in the $[0\ 0\ 1]$ direction transforms into a Fe-

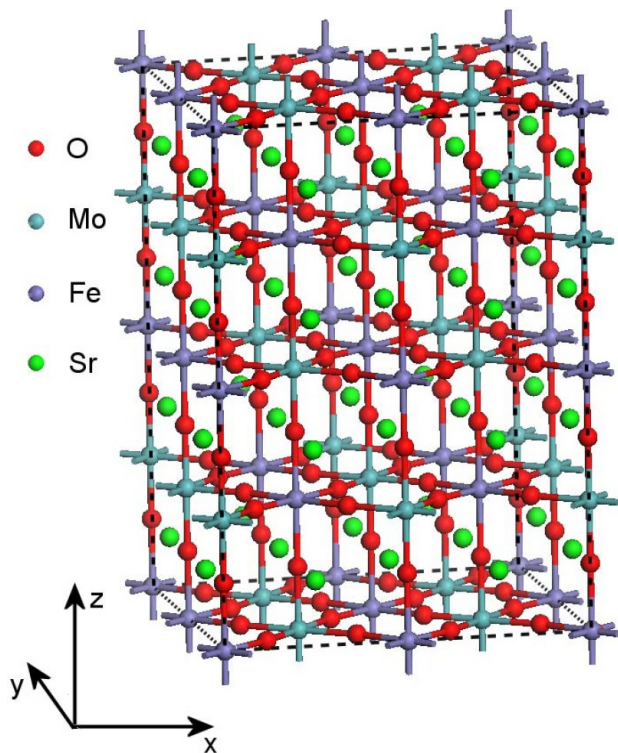


FIGURE 1. (Color online) Supercell structure for $\text{Sr}_2\text{FeMoO}_6$. For each of the eight unit cells used to built up this supercell it is possible to identify that Fe is located at every vertex and at the center of the cell while Mo atoms are at the center of top and bottom faces, as well as at the center of every edge. Between every Fe-Mo nearest neighbor couple there is an O atom; the remains are Sr atoms.

O-Fe-O-Fe-O-Fe-O- chain. For the third supercell (C) there are two consecutive Mo-O-Fe-O-Fe-O-Fe-O- chains in the $[0\ 0\ 1]$ direction at the $(0\ 4\ 0)$ supercell plane, producing 12.5% more Fe than Mo content as compared to the (B) supercell. The fourth supercell (D) contains a Fe-O-Fe-O-Fe-O-Fe-O-chain and a Mo-O-Fe-O-Fe-O-Fe-O- chain as it represents simultaneously the (A) and (B) cases. Finally, in the supercell (E) there are two parallel Fe-O-Fe-O-Fe-O-Fe-O- chains and this supercell is 25% richer in Fe than Mo.

3. Results and discussions

We confirm that the alpha (up spin) valence band of $\text{Sr}_2\text{FeMoO}_6$ is composed by e_g and t_{2g} electrons from Fe and Mo atoms, as reported previously [1,14], but we found that they are distributed at separate bonding and antibonding peaks (Fig. 2). Mandal *et al.* [14] assign Fe e_g and t_{2g} states only at the valence band and Mo t_{2g} ones at the conduction band; in contrast, we observe the existence of e_g and t_{2g} bonding contributions of both atoms within the valence band, and these states are unfolded by combination with p_x and p_y oxygen states.

The behavior of the alpha channel is due to the strong splitting among bonding and antibonding d states, being the latter above the Fermi level [13-15]. For the conducting beta (down spin) channel around the Fermi level, we found a t_{2g} bonding state for Fe in the valence band, almost at the Fermi level, as well as e_g and t_{2g} Fe states which are bonding and antibonding respectively, the latter at higher energy. Although, the valence band is composed of bonding combinations of d electrons, a peak at the top of this band is built by antibonding Fe e_g states; thus, when one Mo is replaced by Fe, the energy gap is weakened, *i.e.*, spin correlation is diminished by the new Fe located in an antisite, where the spin node associated with the Mo disappears.

The electronic configurations of Mo and Fe atoms are $[\text{Kr}]5s^24d^4$ and $[\text{Ar}]4s^23d^6$ respectively, *i.e.*, it is expected

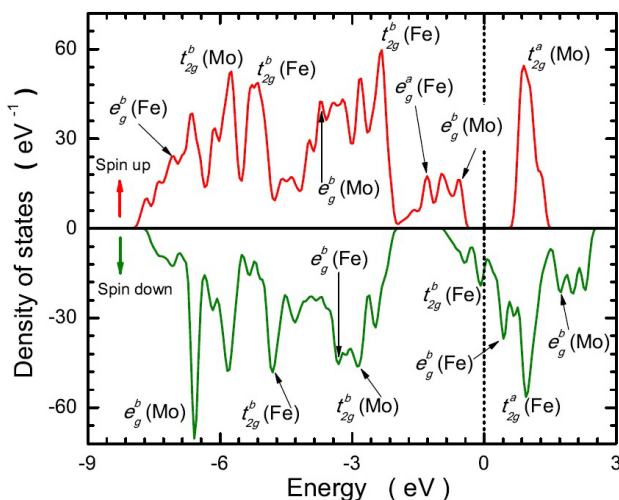


FIGURE 2. (Color online) Total density of states of $\text{Sr}_2\text{FeMoO}_6$ around the Fermi level (vertical dotted line). The orbital symmetry labels are included.

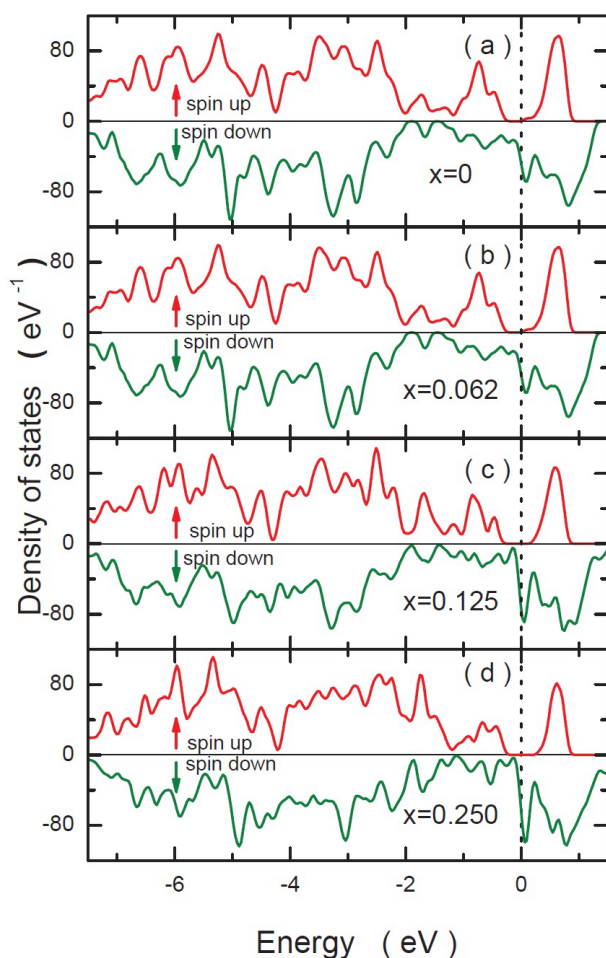


FIGURE 3. (Color online) DOS of $\text{Sr}_2\text{Fe}_{1+x}\text{Mo}_{1-x}\text{O}_6$ for majority and minority spins for $x = 0$ (a), 0.0625 (b), 0.125 (c) and 0.250 (d). The difference among compounds resides on the amount and specific places where Mo atoms are replaced by Fe, constituting different configurations.

that the number of electronic states around the Fermi level increases with x due to the injection of Fe 3d electrons to the lattice (Fig. 3). This injection has different effects on alpha and beta channels: on the top of the valence band for the conducting alpha channel new states are generated which further develop a band occupying the energy gap region, whereas the band for the conducting beta channel is shifted to lower energies due to the occupation of states above the Fermi level.

For the same concentration ($x = 0.125$) but different antisite replacement configurations, the energy gap for the up-spin channel as well as the distribution of accessible states are not appreciably modified. That is the case for the supercells (B) and (C); the total density of states for the former is shown (Fig. 3c), corresponding to $x = 0.125$. Figure 3 shows our spin-polarized calculations for the total density of states from $x = 0.0$ to $x = 0.25$ in $\text{Sr}_2\text{Fe}_{1+x}\text{Mo}_{1-x}\text{O}_6$, and the half-metallic ground state in agreement with experiments [9].

4. Conclusions

In summary, we have studied the off-stoichiometric $\text{Sr}_2\text{Fe}_{1+x}\text{Mo}_{1-x}\text{O}_6$ system for $x > 0$ compositions using first-principles calculations. For the stoichiometric compound ($x = 0$), it is found that valence and conducting bands are formed by bonding and antibonding crystalline orbitals arising from combinations of Fe and Mo d orbitals with O p ones. It is also found that the system has a half-metallic ferromagnetic ground state.

Acknowledgements

This work was partially supported by Grant-57929 from CONACyT, PAPIIT-IN108710 from UNAM and Multidisciplinary Project SIP-IPN-1439. E. Carvajal would like to thank the financial support from CONACyT.

1. K.-I. Kobayashi, T. Kimura, H. Sawada, K. Terakura, and Y. Tokura, *Nature* **395** (1998) 677.
2. S. Nakayama, T. Nakagawa, and S. Nomura, *J. Phys. Soc. Japan* **24** (1968) 219.
3. Cz. Kapusta *et al.*, *J. Mag. Mag. Mater.* **242** (2002) 701.
4. M.T. Causa, A. Butera, M. Tovar, and J. Fontcuberta, *Physica B* **320** (2002) 79.
5. M.S. Moreno *et al.*, *Physica B* **320** (2002) 43.
6. S. Ray, A. Kumar, S. Majumdar, E.V. Sampathkumaran, and D.D. Sarma, *J. Phys. Condens. Matter.* **13** (2001) 607.
7. E. Carvajal, O. Navarro, R. Allub, M. Avignon, and B. Alascio, *Eur. Phys. J. B* **48** (2005) 179.
8. B. Aguilar, O. Navarro, and M. Avignon, *Eur. Phys. Lett.* **88** (2009) 67003.
9. D. Topwal, D.D. Sarma, H. Kato, Y. Tokura, and M. Avignon, *Phys. Rev. B* **73** (2006) 094419.
10. J.P. Perdew, K. Burke, and M. Ernzerhof, *Phys. Rev. Lett.* **77** (1996) 3865.
11. S.J. Clark *et al.*, *Zeitschrift fuer Kristallographie* **220** (2005) 567.
12. Accelrys Inc., *CASTEP Users Guide* (San diego, Accelrys Inc. 2001).
13. X.F. Zhu, Q.F. Li, and L.F. Chen, *J. Phys.: Condens. Matter* **20** (2008) 075218.
14. T.K. Mandal, C. Felser, M. Greenblatt, and J. Kübler, *Phys. Rev. B* **78** (2008) 134431.
15. P. Sanyal, H. Das, and T. Saha-Dasgupta, *Phys. Rev. B* **80** (2009) 224412.